



Pharmacokinetics of a synthetic interferon inducer amixin in mice

Vladimir G. Zinkovsky¹, Olga V. Zhuk¹, Svetlana K. Sumriy²

¹Department of Biotechnology and Molecular Biology, University of Opole, Kominka 4, PL 45-035 Opole, Poland

²Department of Biology, Odessa National University, Dvoryanskaya 2, 65000 Odessa, Ukraine

Correspondence: Olga V. Zhuk, e-mail: olga_zhuk@uni.opole.pl

Abstract:

Pharmacokinetics of amixin, a synthetic interferon inducer, has been studied in mice under intravenous and oral routes of administration. Following oral administration, 80% of the drug was eliminated in the unchanged form. Its absolute biological availability comprised 0.7. In comparison to oral administration, after intravenous injection concentrations of amixin and its radioactive metabolites were higher during the first 5–120 min of the experiment in all organs and tissues. During the first 4–24 h, we observed an increase in the total radioactive material that was similar for both modes of administration. Low drug elimination rate was noted under both conditions. A novel integral model-independent method for estimation of equilibrium tissue-to-plasma partition ratios (K_p) has been proposed. The suggested integral parameter K_p does not depend on the structure of the kinetic scheme and, most importantly, could be used for analysis of incomplete kinetic curves. We also propose a combined model that could help determine parameters of irreversible xenobiotic binding, the extent of the absorption from the intestine and relative efficacy of the hepatic excretion, in particular presystemic drug elimination.

Key words:

amixin (tilorone), distribution, xenobiotic mass transfer, area under curve

Introduction

Amixin or tilorone (2,7-bis-[2-N,N-diethylaminoethoxy]-fluorene-9-one) is a synthetic immunomodulator widely used in therapy and prophylaxis of viral diseases [13, 24, 31–33]. Antiviral and interferon-inducing action of tilorone has been known for more than 30 years [8–10]. According to numerous studies [7, 17, 18, 20, 23, 30, 34, 35, 38, 44], tilorone stimulates production of endogenous interferon mainly in T-lymphocytes. Binding of interferons to their specific receptors initiates synthesis of antiviral, antiproliferative and immunomodulating substances [4, 6,

26, 28, 40, 46]. Antiviral activity of tilorone against hepatitis B and C viruses has received a particular attention [13, 17, 39]. Activation of spleen natural killer cells *in vivo* has been documented and a possibility of using tilorone as a cytostatic drug was discussed [1–3, 25, 27, 29]. One of the possible mechanisms of antiviral effects of tilorone could involve its interaction with nucleic acids [8–10, 21, 37]. Tilorone and similar compounds could, therefore, have an oncotherapeutic potential [5, 12, 22].

In contrast to many studies on the biological activity and mechanisms of action of tilorone, there are very few accounts of its pharmacokinetics in animals. Wacker et al. have studied distribution of the total

radioactivity after intraperitoneal administration of ^{14}C -tilorone at a single dose of 1.5 mg/kg and only after 16 h [45]. Maximum contents of tilorone were determined in the liver, spleen and kidneys of mice. Gaur and Chandra who studied distribution of tilorone 24 h after its administration have obtained similar results [15]. Intracellular distribution of [^{14}C]-tilorone hydrochloride in various tissues of rats and mice was also reported in the latter study. Golovenko and Boriyuk studied pharmacokinetics of amixin following multiple oral administration [19]. They noted a high steady-state concentration of the drug in various tissues and its slow elimination. It has been demonstrated that biotransformation of tilorone in rats and mice is not significant [41, 45]. Minor metabolites detected in the above-mentioned studies were products of oxidation of aliphatic moieties of the tilorone molecule. Depending on the biosubstrate, 70–90% of the total radioactivity was represented by the parent drug [41, 45]. This allows for using kinetics of the total radioactivity contents for pharmacokinetic studies of [^3H]-tilorone.

In our study, we, therefore, studied kinetics of [^3H]-amixin distribution in tissues of mice following a single intravenous or oral administration. Since elimination of amixin is very slow, we proposed a novel integral method of model-independent analysis that could be used to analyze pharmacokinetics of xenobiotics that lack a pronounced distribution or elimination phase. Also a combined model-independent method has been worked out to determine irreversible binding of amixin in the body.

Materials and Methods

The study was conducted according to the principles of the “Declaration of Helsinki”. Experimental protocols were approved by the Ethics Committee of the Pharmacological Committee of Ukraine and performed in strict accordance with the Ethics Committee regulations for the use of experimental animals.

Animals

The experiments were performed on female outbred mice weighing 18–24 g. The animals were obtained from the breeding facility of the Russian Academy of

Medical Sciences (“Stolbovaya”, Moscow, Russia) and housed in groups of eight to ten animals per cage. The mice were kept under a continuous 12 h light-dark cycle at the room temperature and were provided with food and water *ad libitum*.

Experimental procedures

Pharmacokinetics of amixin was studied using labeled 2,7-bis-[2-N,N-diethylamino- ^3H]-ethoxy]-fluorene-9-one dihydrochloride (I) (JSC Interkhim, Odessa, Ukraine). High radiochemical purity of [^3H]-I (99.6%) was inferred from radiochromatographic analysis and specific radioactivity was 2.3 Ci/mol.

Amixin was administered intravenously in an isotonic solution into caudal vein and orally at a dose of 50 mg/kg. Animals were killed by rapid decapitation at 5, 15, 30 min, 1, 2, 4, 8 and 24 h after administration and their organs and tissues were taken for analysis. Total radioactivity was determined in 0.3 ml samples of plasma and tissue homogenates (1:5) using Tri Carb 2700 scintillation counter (Canberra Packard, USA).

Data analysis

Calculations of total radioactivity in the body after injection of [^3H]-I (mean \pm SEM) and regression analysis were performed using Microsoft Excel. Values of the areas under the “drug concentration–time” curves (AUC_{0-t}) were calculated by the trapezoidal rule. Values of total radioactivity in tissues were compared by Student’s *t*-test for unpaired data. The results were considered to be statistically significant when $p < 0.05$.

Results

Amixin was rapidly distributed in the body upon both ways of administration (Tab. 1). A rapid phase of distribution of [^3H]-I has been noted that faded already during the first hour following drug administration. The highest total radioactivity was observed in the liver and kidneys of mice. The lowest radioactive counts have been found in plasma (Tab. 1). The concentration of [^3H]-I and its radioactive metabolites in the liver was two orders of magnitude higher than in blood throughout the whole study period. Elimination

Tab. 1. The contents of the total radioactive material (DPM*10³/g(ml)) in organs and tissues of mice in the interval of 0.083–24 h after intravenous and oral administration of [³H]-I in a dose 50 mg/kg

Time (h)	Intravenous administration							
	Spleen	Brain	Liver	Kidneys	Muscle	Heart	Lungs	Plasma
0.083	17.8 ± 0.24	23.5 ± 4.08	32.0 ± 6.94	83.0 ± 21.76	21.3 ± 5.82	77.8 ± 17.67	115.9 ± 55.45	
0.25	35.0 ± 5.67	25.4 ± 2.89	64.0 ± 7.76	88.6 ± 11.37	29.1 ± 3.02	87.3 ± 19.20	177.3 ± 21.56	
0.5	43.5 ± 6.78	26.35 ± 4.01	78.4 ± 8.33	109.3 ± 11.85	21.8 ± 2.99	61.5 ± 14.66	103.1 ± 16.99	6.10 ± 2.18
1	51.0 ± 7.82	25.35 ± 3.72	74.9 ± 8.27	86.4 ± 13.94	18.8 ± 2.98	38.8 ± 9.69	60.5 ± 12.96	0.73 ± 0.11
2	77.4 ± 8.24	29.55 ± 1.39	119.7 ± 9.80	119.0 ± 21.89	27.068 ± 2.58	47.3 ± 5.09	75.1 ± 7.83	1.13 ± 0.35
4	51.4 ± 6.19	31.3 ± 5.2	125.8 ± 4.61	91.5 ± 7.12	25.8 ± 2.77	30.1 ± 3.86	68.3 ± 12.87	0.81 ± 0.098
6	35.6 ± 6.29	17.15 ± 2.96	126.2 ± 18.01	92.1 ± 16.14	22.4 ± 4.25	35.3 ± 4.97	44.1 ± 8.95	0.42 ± 0.045
8	65.5 ± 14.02	16.6 ± 2.13	124.0 ± 11.81	48.9 ± 12.32	18.9 ± 3.63	24.8 ± 4.28	42.1 ± 15.89	0.81 ± 0.067
24	97.4 ± 7.66	9.55 ± 1.16	74.1 ± 4.75	26.0 ± 4.66	16.2 ± 2.53	13.5 ± 2.52	31.6 ± 2.79	0.29 ± 0.037

Time (h)	Oral administration							
	Spleen	Brain	Liver	Kidneys	Muscle	Heart	Lung	Plasma
0.25	12.5 ± 6.08	2.2 ± 0.44	103.3 ± 6.81	15.8 ± 1.89	4.0 ± 0.32	9.1 ± 0.80	19.6 ± 1.55	0.50 ± 0.10
0.5	14.2 ± 2.74	3.2 ± 0.483	95.0 ± 20.98	16.55 ± 3.25	3.0 ± 0.71	6.7 ± 0.99	18.8 ± 1.75	0.29 ± 0.08
1	36.1 ± 5.78	1.7 ± 0.404	86.6 ± 14.72	19.8 ± 2.98	5.9 ± 1.31	13.3 ± 2.54	19.7 ± 3.33	0.47 ± 0.13
2	49.0 ± 5.56	7.1 ± 0.62	153.8 ± 22.08	29.84 ± 3.70	7.4 ± 1.19	13.3 ± 0.62	21.3 ± 2.74	0.43 ± 0.07
4	36.6 ± 3.35	11.1 ± 0.99	2011.9 ± 7.12	54.17 ± 5.87	10.6 ± 1.62	26.1 ± 4.55	29.2 ± 3.77	0.75 ± 0.17
6	24.9 ± 3.87	8.9 ± 1.64	137.2 ± 11.45	34.0 ± 3.51	8.8 ± 1.62	16.9 ± 1.47	21.3 ± 1.93	0.40 ± 0.06
8	58.1 ± 8.07	11.2 ± 2.35	105.2 ± 14.34	33.6 ± 3.18	9.3 ± 1.86	15.2 ± 1.70	18.4 ± 3.95	0.44 ± 0.06
24	109.5 ± 14.98	16.0 ± 3.17	128.1 ± 9.39	34.6 ± 2.37	16.47 ± 3.34	12.9 ± 1.90	48.3 ± 2.93	0.37 ± 0.03

of the total radioactivity was rather slow during 0.083–24 h after oral administration of [³H]-I. Variations of total radioactivity contents were observed in some tissues during the first intervals of the experiment (0.083–1 h), which were not significant as estimated by Student's *t*-test (Tab. 1). These variations led to humps in the graphs of the relationships between AUC values (see below). A more detailed study of the mechanism of these variations is necessary, which was, however, beyond the scope of our work. The critical observation crucial for our further analysis of the amixin mass transfer between blood and organs was that the ratio of rate constants approached a steady-state value equal to the equilibrium constant.

We noted that in the case of intravenous injection of [³H]-I, total radioactivity in plasma, kidneys, brain, heart and skeletal muscle tissues was significantly higher (*p* < 0.01) than after oral administration. Such differences, however, have not been observed for liver and spleen. In spleen, significant differences in contents of the drug between different ways of administration were noted only during initial 15 and 30 min. The route of administration did not affect amount of amixin in the liver. An interesting feature of amixin pharmacokinetics after intravenous injection was a high level of total radioactivity in lung tissue at the beginning of the experiment (0.083–2 h). This observation possibly indicates first-pass uptake of the drug by lungs. Also, disproportional increase in total radioactivity was noted in spleen tissue (Tab. 1).

Analysis of the distribution of amixin prompted us to divide all tissues studied into three groups. The first group consisted of organs where first-pass effects and uptake were significant, i.e. hepatic and lung tissues. Organs where drug concentrations were proportional to plasma levels, and where practically steady-state levels of total radioactivity have been observed (kidneys, heart and skeletal muscles, brain) belonged to the second group. Spleen tissue represented the third group where disproportional enhancement of total radioactivity with respect to plasma levels was detected.

Model-independent estimation of distribution of amixin in organs and tissues of experimental animals

Model-independent approaches to the analysis of distribution of xenobiotics are based on the most general kinetic parameters that do not depend on the structure

of the kinetic scheme of the mass transfer of substances in the body [16].

In our previous works, the analysis of the distribution of a xenobiotic between blood and tissues was based on the assumption that the rate of change in its contents in an organ ($d(^2A_t)/dt$) is equal to the difference between rate of its transfer from blood (compartment (1) ($^{12}v_t$)) into this organ (compartment (2)) and rate of the reverse process from (2) in (1) described by rate constants (^{12}k and ^{21}k) [42, 43]:

$$\begin{cases} \frac{d(^2A_t)}{dt} = ^{12}v_t - ^{21}v_t \\ ^{12}v_t = ^{12}k \cdot ^1A_t \\ ^{21}v_t = ^{21}k \cdot ^2A_t \\ ^1A_t = ^1V^1C_t \\ ^2A_t = ^2V^2C_t \end{cases} \quad (1)$$

where 1A_t and 2A_t are quantities of drug in compartments (1) and (2) at time *t*, 1V and 2V are apparent distribution volumes in compartments (1) and (2); 1C_t and 2C_t are concentrations of *A* in compartments (1) and (2).

Model-independent approaches to the analysis of results are based on the equation obtained by integration (from 0 to *t*) of Eq. (1):

$$^2A_t = ^{12}k^1V \int_0^t ^1C_t dt - ^{21}k^2V \int_0^t ^2C_t dt \quad (2)$$

When $t \rightarrow \infty$ in the case of a single administration of a xenobiotic, then $^2A_t \rightarrow 0$. Thus, equation (2) becomes simplified and it is possible to define the value of an equilibrium constant of distribution between blood and studied tissue (*Kp*):

$$Kp = \frac{^{12}k^1V}{^{21}k^2V} = \frac{\left(\int_0^\infty ^2C_t dt \right)}{\left(\int_0^\infty ^1C_t dt \right)} \quad (3)$$

This approach is widely used when analyzing results in accordance with the formal apparatus of physiological modeling of distribution processes of drugs in the body [16, 36]. A disadvantage of this method is the need to estimate $\left(\int_0^\infty ^1C_t dt \right)$ and $\left(\int_0^\infty ^2C_t dt \right)$ values based on results obtained in the limited time interval, set by the experimental protocol. To calculate values

of integrals of xenobiotic concentration $\left(\int_0^{\infty} C_t dt \right)$ areas

under pharmacokinetic curves (AUC) are determined in the interval from 0 to t , by the trapezoidal rule.

If mass transfer of substances in the body indeed follows the mechanisms described by Eq. (1), then irrespective of the nature of changes in xenobiotic concentration in blood (1), its quantity transferred into tissue from the starting time ($t = 0$, ${}^2C_0 = 0$) to the time t $\left(\int_0^t {}^{12}v_t dt \right)$ will be:

$$\int_0^t {}^{12}v_t dt = {}^{12}k {}^1V \int_0^t {}^1C_t dt = {}^{12}k {}^1V {}^1AUC_{0-t} \quad (4)$$

where ${}^{12}k$ is the rate constant (expressed in units of time^{-1}) of xenobiotic translation from (1) to (2); ${}^1AUC_{0-t}$ is the area under the concentration-time relationship of the drug in blood (plasma), determined within the interval from time 0 to t .

The quantity of the substance eliminated from (2) (i.e. transferred back to (1) from (2)) at time t is:

$$\int_0^t {}^{21}v_t dt = {}^{21}k {}^2V \int_0^t {}^2C_t dt = {}^{21}k {}^2V {}^2AUC_{0-t} \quad (5)$$

where ${}^{21}k$ is the rate constant of xenobiotic translation from the compartment (2) to (1); ${}^2AUC_{0-t}$ is the area under the concentration-time relationship of the drug in tissue, determined, analogously, within the interval from time 0 to t .

Then, the quantity of the substance present in the tissue (2) at time t (2A_t) is:

$${}^2A_t = {}^2C_t {}^2V = {}^{12}k {}^1V {}^1AUC_{0-t} - {}^{21}k {}^2V {}^2AUC_{0-t} \quad (6)$$

Therefore:

$$\frac{{}^2AUC_{0-t}}{{}^1AUC_{0-t}} = \frac{{}^{12}k {}^1V}{{}^{21}k {}^2V} - \frac{{}^2C_t}{{}^1AUC_{0-t}} \quad (7)$$

The value of $\frac{{}^2C_t}{{}^1AUC_{0-t}}$ from Eq. (7) should approach

zero in the course of the experiment, because the value of 2C_t approaches zero, as $t \rightarrow \infty$, and the value of ${}^1AUC_{0-t} \rightarrow {}^1AUC_{0-\infty}$. Thus, with the increase in time of the experiment, the variable $\frac{{}^2AUC_{0-t}}{{}^1AUC_{0-t}}$ should approach $({}^{12}k {}^1V)/({}^{21}k {}^2V) = K_p$. This

conclusion was confirmed during the analysis of the distribution kinetics of amixin in mice (Fig. 1).

To determine the value of $({}^{12}k {}^1V)/({}^{21}k {}^2V) = K_p$ by regression approach, the following transformation of Eq. 7 could be applied:

$${}^2AUC_{0-t} = \frac{{}^{12}k {}^1V}{{}^{21}k {}^2V} {}^1AUC_{0-t} - \frac{{}^2C_t}{{}^{21}k} \quad (8)$$

Since the variable $\frac{{}^2C_t}{{}^{21}k}$ can be assumed to have

a small value and its change would negligibly affect the determination of the value of $({}^{12}k {}^1V)/({}^{21}k {}^2V)$, it can be defined as a constant (b) in a linear equation:

$${}^2AUC_{0-t} \approx \frac{{}^{12}k {}^1V}{{}^{21}k {}^2V} {}^1AUC_{0-t} + b \quad (9)$$

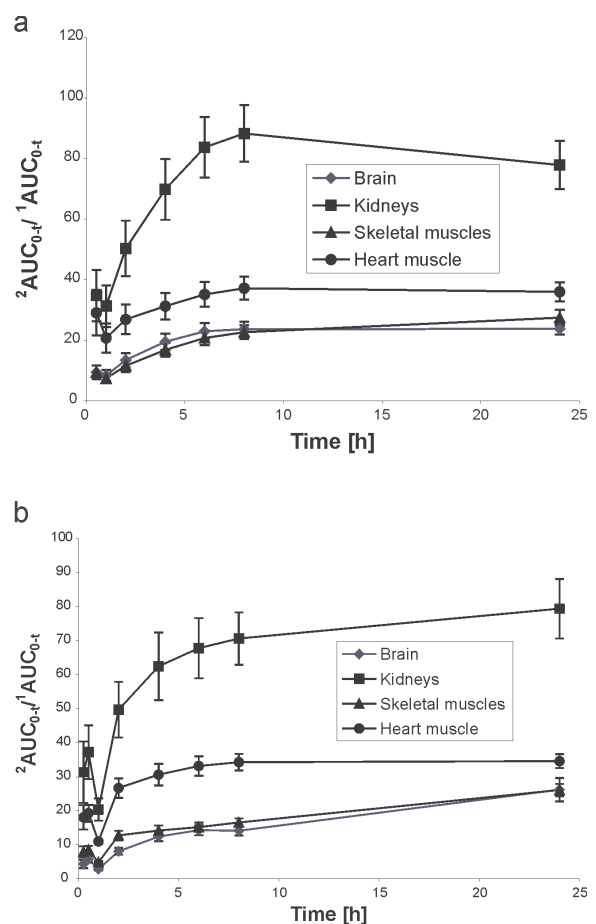


Fig. 1. The ratio between the areas under curves of the contents of total radioactivity in tissue and plasma $\left(\frac{{}^2AUC_{0-t}}{{}^1AUC_{0-t}} \right)$ after intravenous

(a) and oral (b) administration of $[{}^3\text{H}]$ -amixin into mice at a dose of 50 mg/kg as a function of time of the experiment

As seen from Figure 2, this assumption is quite acceptable. The corresponding values of $(^{12}k^1V)/(^{21}k^2V) = K_p$, determined by regression approach are equal to regression coefficients in Figure 2 and asymptotes' values in Figure 1 (abscissa (x) – $^1AUC_{0-t}$; ordinate (y) – $^2AUC_{0-t}$).

As follows from this simple integral model-independent analysis (Figs. 1, 2, Tab. 2), amixin phar-

macokinetics is characterized by higher values of rate constants of its distribution into organs and tissues from blood in comparison to constants of the reverse processes. The ratios of these values are identical at different ways of administration of the drug (Tab. 2). The ratio of AUC values in conditions of oral and intravenous administrations was ≈ 0.6 . This matched similar values determined for plasma (0.7). The ratio between the area under the "concentration–time" relationship of the amixin in plasma for the two routes of administration $(\frac{^{po}AUC_{0-\infty}}{^{iv}AUC_{0-\infty}})$ asymptotically approached the value of absolute bioavailability (F_{abs}).

Determination of the irreversible binding of amixin in the spleen of mice

Combined methods of analysis assume the presence of intercompartmental (mass transfer) and intracompartamental (metabolism, binding) phenomena in the kinetic scheme.

Irreversible binding parameters in various organs and tissues are quintessential for the estimation of drug safety [36]. Therefore, in the present paper, we would like to propose a method based on the following postulates:

1. The amount of a xenobiotic in an organ (tissue) is defined by the difference between integers of the rates of its transfer from blood (1) to an organ and from an organ (2) to blood (1).
2. The rates of mass transfer between the two biophases – blood (1) and an organ (2) studied are proportional to xenobiotic concentrations in them [16].

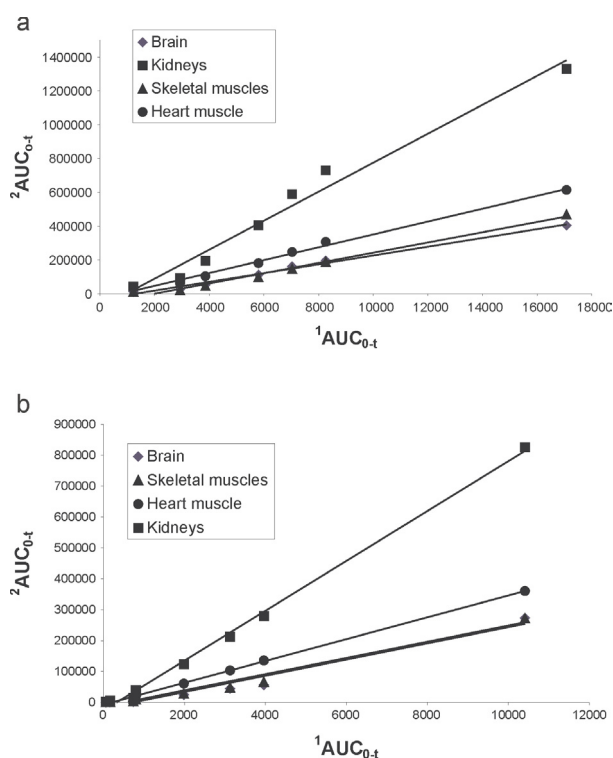


Fig. 2. Correlation between the concentration of $[^3H]$ -amixin/metabolites in tissue ($^2AUC_{0-t}$) and plasma ($^1AUC_{0-t}$) as a function of time after intravenous (a) and oral (b) administration of $[^3H]$ -amixin into mice at a dose of 50 mg/kg

Tab. 2. Model-independent pharmacokinetic parameters of the distribution of amixin in mice after intravenous and oral administration at a dose of 50 mg/kg

Organ	Parameters				$\frac{^2AUC_{(0-24), po}}{^2AUC_{(0-24), iv}}$
	Intravenous administration		Oral administration		
	$^2AUC_{0-24}$ (DPM*10 ³ /g)*h)	K_p	$^2AUC_{0-24}$ (DPM*10 ³ /g)*h)	K_p	
Skeletal muscles	468.4 ± 20.34	30.3 ± 2.13	271.9 ± 18.90	26.2 ± 3.46	0.58 ± 0.10
Heart muscle	613.3 ± 25.65	38.01 ± 3.01	360.4 ± 23.46	35.3 ± 2.67	0.59 ± 0.09
Kidneys	1329.0 ± 10.35	85.7 ± 5.67	826.1 ± 69.75	80.7 ± 4.69	0.62 ± 0.21
Brain	404.4 ± 37.89	26.6 ± 1.28	275.8 ± 28.90	26.4 ± 1.89	0.68 ± 0.11

3. The rate of xenobiotic binding by an organ studied is proportional to the quantity of free (non-bound) substance ($^{free,2}C_t \cdot ^2V$):

$$^{22}v_t = ^{free,2}C_t \cdot ^2V \cdot ^{22}\chi \quad (10)$$

where 2V and $^{22}\chi$ are the volume of an organ and rate constant (first order, dimensionality – [time] $^{-1}$) of the xenobiotic binding (Fig. 3).

To detect the very fact of irreversible amixin binding to spleen tissue and to estimate parameters of this process, we have worked out the following method.

The ratio of the amixin concentration in spleen to its concentration in plasma increased practically linearly during the time of experiment (Fig. 4). This could be due to irreversible binding of amixin to tissues or

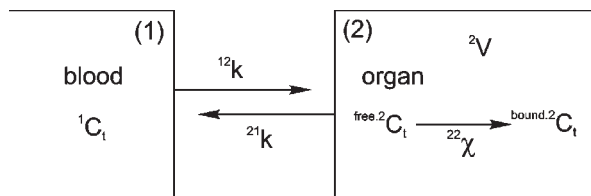


Fig. 3. The mass transfer of xenobiotic between blood (compartment 1) and studied organ that takes into account irreversible binding to an organ (compartment 2)

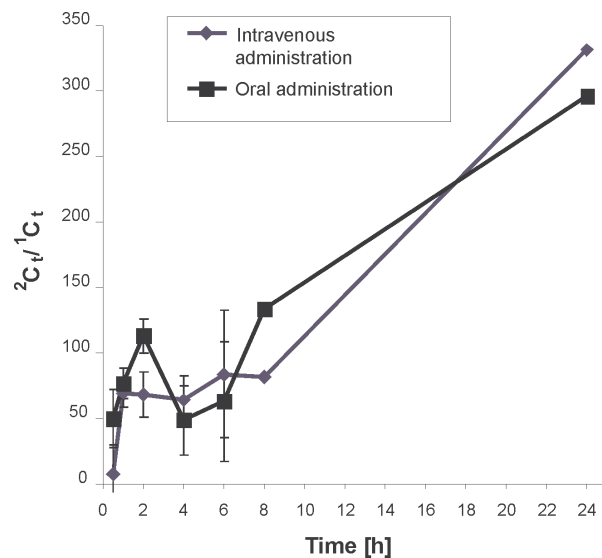


Fig. 4. Temporal dependence of the ratio between the levels of total radioactivity in spleen (2C_t) and plasma (1C_t) after intravenous and oral administration of [3H]-amixin into mice at a dose of 50 mg/kg

to the fact that the ratio of rate constants of the onward and backward processes is large, while the characteristic times (the backward values of rate constants of these processes) of them significantly exceeded the experimental time of observation [47].

On the basis of the above-mentioned postulates, the quantity of the irreversibly bound drug ($^{bound,2}C_t$) at time t is:

$$\begin{aligned} ^{bound,2}C_t \cdot ^2V &= ^{22}\chi \cdot ^2V \int_0^t ^{22}v_t dt = \\ &= ^{22}\chi \cdot ^2V \cdot ^{free,2}AUC_{0-t} \end{aligned} \quad (11)$$

where $^{free,2}AUC_{0-t}$ is the area under the pharmacokinetic concentration-time relationship of the free (unbound) drug in tissue.

Therefore:

$$^{bound,2}C_t = ^{free,2}AUC_{0-t} \cdot ^{22}\chi \quad (11a)$$

The concentration of the free drug, ($^{free,2}C$) cannot be determined directly, so total contents of free and bound drug is usually determined experimentally ($^{free,2}C_t + ^{bound,2}C_t$). However, it follows from the Figure 3 and Eqs. (7) and (8) that:

$$\begin{aligned} ^{free,2}C_t \cdot ^2V &= ^1AUC_{0-t} \cdot ^{12}k \cdot ^1V - ^{free,2}AUC_{0-t} \cdot \\ ^2V \cdot (^{21}k + ^{22}\chi) \end{aligned} \quad (12)$$

where $^{12}k \cdot ^1V \cdot ^1AUC_{0-t} = \int_0^t ^{12}v_t dt$.

Substitution of (11a) into (12) results in:

$$\begin{aligned} \left(^{free,2}C_t + ^{bound,2}C_t \right) \cdot ^2V &= ^1AUC_{0-t} \cdot ^{12}k \cdot ^1V - \\ - ^{free,2}AUC_{0-t} \cdot ^{21}k \cdot ^2V \end{aligned}$$

$$\left(^{free,2}C_t + ^{bound,2}C_t \right) = \frac{^1AUC_{0-t} \cdot ^{12}k \cdot ^1V}{^2V} - ^{free,2}AUC_{0-t} \cdot ^{21}k \quad (13)$$

$$\left(\frac{^{free,2}C_t + ^{bound,2}C_t}{^1AUC_{0-t}} \right) = \frac{^{12}k \cdot ^1V}{^2V} - \frac{^{free,2}AUC_{0-t} \cdot ^{21}k}{^1AUC_{0-t}} \quad (14)$$

$$At \ t \rightarrow \infty \quad ^{free,2}AUC_{0-\infty} \rightarrow ^1AUC_{0-\infty} \cdot \frac{^{12}k \cdot ^1V}{(^{21}k \cdot ^{22}\chi) \cdot ^2V}$$

Then:

$$\left(\frac{free,2C_{\infty} + bound,2C_{\infty}}{{}^1AUC_{0-\infty}} \right) = \frac{{}^{12}k^1V}{2V} - \frac{1V}{2V} \left(\frac{{}^{12}k^21k}{{}^{21}k + {}^{22}\chi} \right) = \frac{{}^{12}k^1V}{2V} - \frac{{}^{12}k^1V}{2V} \left(\frac{{}^{21}k}{{}^{21}k + {}^{22}\chi} \right) \quad (15)$$

Since at $t \rightarrow \infty$ value $free,2C_{\infty} \rightarrow 0$, the quantity of bound drug can be estimated from the graph with coordinates $\left(\left(\frac{{}^2C_t}{{}^1AUC_{0-t}} \right), t \right)$ (Fig. 5). At $t \rightarrow 0$ the

curve crosses the ordinate in the point equal to $\frac{{}^{12}k^1V}{2V}$ and asymptotically approaches the value $\frac{{}^{12}k^1V}{2V} \left(\frac{{}^{21}k}{{}^{21}k + {}^{22}\chi} \right)$ with time. The former value

($\frac{{}^{12}k^1V}{2V}$) can be estimated at $\approx 300 \text{ h}^{-1}$, while the latter is within $3-8 \text{ h}^{-1}$. Thus, relative efficiency of the irreversible binding $\left(\frac{{}^{21}k}{{}^{21}k + {}^{22}\chi} \right)$ is approximately

1–2%.

In other words, almost 98–99% of the drug that is taken up by the spleen is eliminated back to plasma, while 1–2% irreversibly binds to the tissue. Nonetheless, even such a seemingly ineffective process significantly affects the kinetics of contents of $[^3\text{H}]$ -products in the spleen (Tab. 1, Fig. 5). This is explained by a high rate of the on- and backward mass transfer of amixin in the “spleen-blood” system.

No significant irreversible binding of amixin has been observed in other organs.

The estimation of the degree of absorption of amixin from the intestine, its presystemic elimination and first-pass effect

To assess the absorption of amixin from the intestine, relative hepatic excretion and, in particular, presystemic elimination, we have compared kinetics of its contents in the plasma and liver upon its administration *via* intravenous and oral routes. As could be seen from Table 1, the contents of the drug in the liver are more than two orders of magnitude higher than its contents in blood during the whole experimental period. This may indicate a significant hepatic excretion, including presystemic one, even at low values of the rate constant of amixin excretion with bile ($el, bilk$).

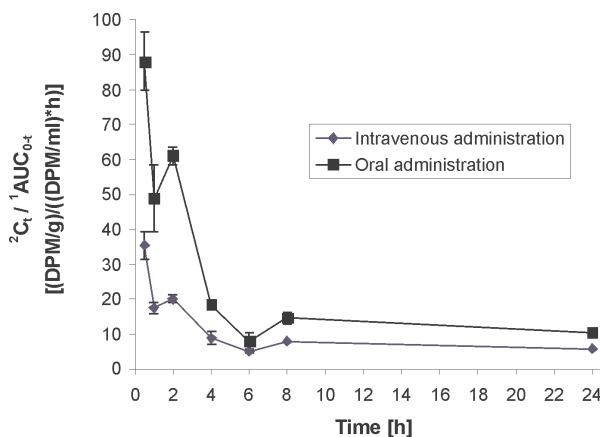


Fig. 5. The ratio between concentrations of amixin and its metabolites (2C_t) in spleen and areas under curves of total radioactivity (${}^1AUC_{0-t}$) in plasma as a function of time after intravenous and oral administration of $[^3\text{H}]$ -amixin into mice at a dose of 50 mg/kg

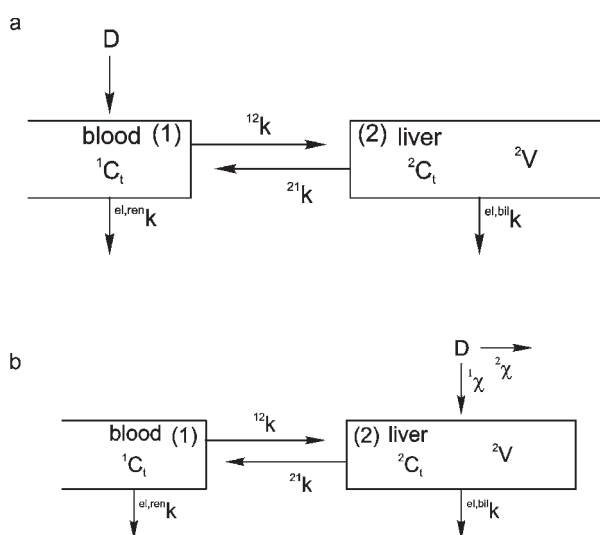


Fig. 6. The scheme of the distribution of amixin between blood and liver during intravenous (a) and oral (b) administration into mice

Formal framework of the analysis

Biological availability of amixin was ≈ 0.7 . Principal kinetic scheme of the distribution and elimination of the drug under conditions of intravenous (a) and oral (b) administrations is presented in Figure 6.

Since plasma (compartment 1) is reversibly connected to other organs with unknown volumes, values of distribution and on/off- rate constants, it is de-

picted as an open compartment of an indefinite volume. The known values are concentrations of amixin in plasma (1C_t) at various time points (t). It is assumed that renal excretion takes place from this compartment with the rate constant ${}^{el,ren}k$. This is the only excretion route from plasma. Also, plasma is reversibly linked with the liver (compartment 2) by mass transfer of amixin that is characterized by rate constants ${}^{12}k$ and ${}^{21}k$. Hepatic excretion with bile is described by the rate constant ${}^{el,bil}k$. Following oral administration (Fig. 6b) amixin enters hepatportal system with the rate constant ${}^1\chi$ and, consequently, into the liver. At the same time, the fraction of the drug that was not absorbed during the passage through the intestine is excreted with feces (rate constant ${}^2\chi$).

“Complete” uptake into the liver after oral administration (F_1) is given by:

$$F_1 = \frac{{}^1\chi}{{}^1\chi + {}^2\chi} \quad (16)$$

Having entered into hepatportal system, fraction of the drug ${}^{po}D$ equal to

$${}^{po}D_1 = {}^{po}D F_1 \quad (17)$$

undergoes two parallel processes, namely entry into circulatory system and presystemic elimination. The dose of the drug entering circulation (${}^{po}D_2$) is given by:

$${}^{po}D_2 = {}^{po}D_1 \frac{{}^{21}k}{{}^{21}k + {}^{el,bil}k} \quad (18)$$

where $\frac{{}^{21}k}{{}^{21}k + {}^{el,bil}k} = F_2$ is relative efficiency of the mass transfer from the liver (compartment 2) into blood (compartment 1):

$$F_{abs} = F_1 F_2 \quad (19)$$

$${}^{po}D_2 = {}^{po}D F_{abs} = {}^{po}D F_1 F_2 \quad (20)$$

$$F_{abs} = \frac{{}^{iv}D}{{}^{po}D} \frac{{}^1AUC_{{}^{po}0-\infty}}{{}^1AUC_{{}^{iv}0-\infty}} = \frac{{}^1\chi}{{}^1\chi + {}^2\chi} \cdot \frac{{}^{21}k}{{}^{21}k + {}^{el,bil}k} \quad (21)$$

Some fraction of the drug in the hepatportal system undergoes presystemic elimination:

$${}^{po}D_3 / {}^{po}D = (1 - F_2) F_1 = \frac{{}^1\chi}{{}^1\chi + {}^2\chi} \cdot \frac{{}^{el,bil}k}{{}^{21}k + {}^{el,bil}k} \quad (22)$$

The utilization of the formal framework of the diffusion modeling allows for calculation of the values presented in Eqs. (15–22) on the basis of experimental data (Tab. 1) and the following considerations [43]:

1. Upon intravenous administration the amount of the drug transferred into the liver from blood at time t is: ${}^1AUC_{{}^{iv}0-t} {}^{12}k {}^1V$.

2. The amount of amixin transferred back to blood from the liver is: ${}^2AUC_{{}^{iv}0-t} {}^{21}k {}^2V$.

3. The amount of amixin excreted from the liver with bile is: ${}^2AUC_{{}^{iv}0-t} {}^{el,bil}k {}^2V$.

Consequently, after time t , following the administration of amixin, its concentration in the liver (${}^2C_t^{iv}$) would be:

$${}^2C_t^{iv} = \frac{{}^{12}k {}^1V}{{}^2V} {}^1AUC_{{}^{iv}0-t} - ({}^{21}k + {}^{el,bil}k) ({}^2AUC_{{}^{iv}0-t}) \quad (23)$$

Then the plot of the relationship ${}^2AUC_{{}^{iv}0-t} / {}^1AUC_{{}^{iv}0-t}$ versus t (Fig. 7) asymptotically approaches

$$\frac{{}^{12}k {}^1V}{({}^{21}k + {}^{el,bil}k) {}^2V} : \frac{{}^2AUC_{{}^{iv}0-t}}{{}^1AUC_{{}^{iv}0-t}} = \frac{{}^{12}k {}^1V}{({}^{21}k + {}^{el,bil}k) {}^2V} - \frac{{}^2AUC_{{}^{iv}0-t}}{({}^{21}k + {}^{el,bil}k) {}^1AUC_{{}^{iv}0-t}} \quad (24)$$

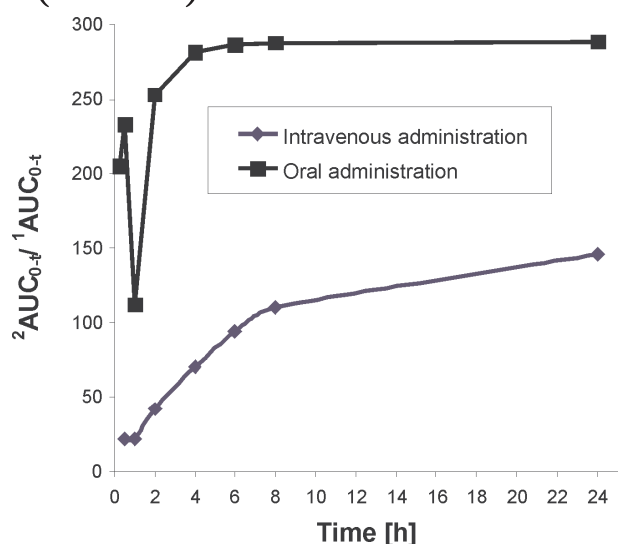


Fig. 7. The ratio between the areas under curves of the content of total radioactivity in liver and plasma after intravenous and oral (${}^2AUC_{{}^{iv}0-t} / {}^1AUC_{{}^{iv}0-t}$) administration of amixin into mice at a dose of 50 mg/kg as a function of time of the experiment

as the value of ${}^2C_t / {}^1AUC_{0-t}^{iv} \rightarrow 0$ at $t \rightarrow \infty$.

By means of the regression analysis of the experimental data (Fig. 8) according to the Eq. (24) the value $\frac{{}^{12}k {}^1V}{({}^{21}k + {}^{el,bil}k) {}^2V}$ was found to be equal to 154.

4. Under oral administration of a dose of amixin D , it is $F_1 * D$ that actually enters hepatoportal system. It is not a sole source from which amixin is transferred to blood: the fraction of the drug, which was transferred back from the liver into blood, undergoes reversible transfer to organs and tissues. Also, amixin is excreted from blood *via* renal route with the rate constant ${}^{el,ren}k$.

Therefore, concentration of amixin in plasma (${}^1C_t^{po}$) at time t after its oral administration can be given by the following equation:

$${}^1C_t^{po} {}^1V = {}^2AUC_{0-t}^{po} \cdot {}^{21}k {}^2V - {}^1AUC_{0-t}^{po} {}^1V ({}^{el,ren}k + {}^{12}k) + \left[\sum_{i=3}^{i=n} {}^i AUC_{0-t}^{po} \cdot {}^i V {}^i k - {}^i V {}^1 AUC_{0-t}^{po} \sum_{i=3}^{i=n} {}^i k \right] \quad (25)$$

where the term within square brackets corresponds to the unknown quantity of amixin that is located at time t in organs and tissues reversibly linked to plasma by mass transfer processes with the rate constants ${}^i k$ and ${}^i k$. Those organs and tissues are not shown in Fig. 6, consequently plasma is depicted as being open. Therefore:

$$\frac{{}^2 AUC_{0-t}^{po}}{{}^1 AUC_{0-t}^{po}} = \frac{({}^{12}k + {}^{el,ren}k) {}^1V}{{}^{21}k {}^2V} + \frac{{}^1 C_t^{po}}{{}^{21}k {}^1 AUC_{0-t}^{po}} - \frac{\left[\sum_{i=3}^{i=n} {}^i AUC_{0-t}^{po} \cdot {}^i V {}^i k - {}^i V {}^1 AUC_{0-t}^{po} \sum_{i=3}^{i=n} {}^i k \right]}{{}^{21}k {}^1 AUC_{0-t}^{po}} \quad (26)$$

5. Both the value of 1C_t and terms of Eq. (25) and (26) in square brackets approach zero in the course of the experiment. Thus (Fig. 7), the value $\frac{{}^2 AUC_{0-t}^{po}}{{}^1 AUC_{0-t}^{po}}$ asymptotically approaches the value of $\frac{({}^{12}k + {}^{el,ren}k) {}^1V}{{}^{21}k {}^2V}$, that could be found (Fig. 8) from the Eq. (25) and was equal to 294.

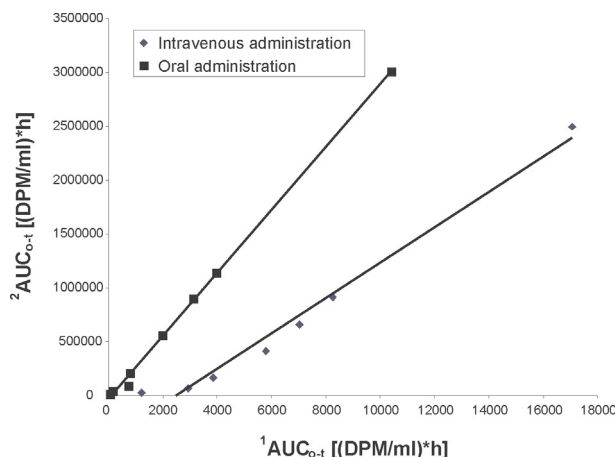


Fig. 8. Correlation between the concentration of $[^3\text{H}]$ -amixin/metabolites in the liver (${}^2AUC_{0-t}$) and plasma (${}^1AUC_{0-t}$) as a function of time after intravenous and oral administration of $[^3\text{H}]$ -amixin into mice at a dose of 50 mg/kg

6. Since the excretion rate constants are usually one or two orders of magnitude lower than the rate constants describing the reversible mass transfer of xenobiotics between blood and tissues, we can assume that:

$$\sqrt{\frac{{}^{12}k {}^1V {}^2}{({}^{21}k + {}^{el,bil}k) {}^2V}} \frac{({}^{12}k + {}^{el,ren}k)}{{}^{21}k {}^2V} \approx \frac{{}^{12}k {}^1V}{{}^{21}k {}^2V} \approx \sqrt{\frac{{}^2 AUC_{0-\infty}^{iv}}{({}^1 AUC_{0-\infty}^{iv})}}{\frac{{}^2 AUC_{0-\infty}^{po}}{({}^1 AUC_{0-\infty}^{po})}}} \quad (27)$$

where terms in brackets are asymptotes of the Fig. 8. The value ${}^{12}k / {}^{21}k \approx 200$.

Then:

$$\frac{\left[\frac{{}^2 AUC_{0-\infty}^{iv}}{({}^1 AUC_{0-\infty}^{iv})} \right]}{{}^{21}k} \bigg/ \sqrt{\frac{{}^2 AUC_{0-\infty}^{iv}}{({}^1 AUC_{0-\infty}^{iv})} \frac{{}^2 AUC_{0-\infty}^{po}}{({}^1 AUC_{0-\infty}^{po})}} \approx \frac{1}{{}^{21}k + {}^{el,bil}k}} \approx F_2 \approx 0.77.$$

Since $F_{abs} = F_1 * F_2$ was ≈ 0.7 , we could assume that $F_1 \approx 0.9$, i.e. amixin is almost fully absorbed from the intestine into the body after its oral administration.

7. Presystemic elimination of amixin is: ${}^{po}D_3 = {}^{po}D F_1 (1 - F_2) \approx 0.21 {}^{po}D$.

8. It is also possible to estimate the ratio of the values of hepatic and renal clearance (${}^{el,bil}k {}^2V / {}^{el,ren}k {}^1V$):

$$\frac{el, bil k^2 V}{el, ren k^1 V} = \left(\frac{1/154 - 1/200}{294 - 200} \right) \cdot 200 = 0.0032$$

and to predict the ratio of the amixin quantities that are excreted with feces and urine under intravenous $\left[\left({}^{ur} B_{0-\infty}^{iv} \right), \left({}^{fe} B_{0-\infty}^{iv} \right) \right]$ and oral $\left[\left({}^{ur} B_{0-\infty}^{po} \right), \left({}^{fe} B_{0-\infty}^{po} \right) \right]$ administrations:

$$\frac{{}^{ur} B_{0-\infty}^{iv}}{{}^{fe} B_{0-\infty}^{iv}} = \frac{el, bil k^2 V}{el, ren k^1 V} \cdot \frac{{}^2 AUC_{0-\infty}^{iv}}{{}^1 AUC_{0-\infty}^{iv}} = 0.0032 \cdot 154 = 0.49$$

$$\frac{{}^{ur} B_{0-\infty}^{po}}{{}^{fe} B_{0-\infty}^{po}} = \frac{el, bil k^2 V}{el, ren k^1 V} \cdot \frac{{}^2 AUC_{0-\infty}^{po}}{{}^1 AUC_{0-\infty}^{po}} = 0.0032 \cdot 294 = 0.94$$

As could be seen from these calculations, the hepatic clearance has a very small value which is negligible compared to the renal clearance, so higher efficiency of the amixin excretion with feces despite a low value of the excretion rate constant of ($el, bil k$) can be explained only by high content of the drug in the organ (liver) excretion (as $\left({}^{fe} B_{0-\infty}^{iv} \right) = {}^{el, bil} k \int_0^t C_t dt$).

Discussion

Our studies demonstrated that amixin was quickly absorbed into systemic circulation after oral administration. Despite a high degree of absorption of the drug from the gastrointestinal system (90%), its absolute biological availability after oral administration was only about 70% possibly as a result of its presystemic elimination from the hepatportal system (21%). High total radioactivity levels were noted in the liver after both oral and intravenous administration of [^3H]-amixin. Availability of the drug to this organ approached unity. This corroborates observations from previous studies that used intraperitoneal administration of tilorone and showed that maximum contents of radioactive material were found in the liver throughout 0.25–16 h after injection [15, 45]. Some studies reported a possible role of hepatocytes in shaping biological response after administration of tilorone [13, 39]. It was also of interest to note the first-pass uptake of amixin by lungs after intravenous administration.

Contents of amixin in the kidneys, brain, skeletal and cardiac muscle changed proportionally to its concentration in plasma. These tissues, with the exception of cardiac muscle, served as peripheral depots. In all experiments, the equilibrium constant of mass transfer processes between blood stream and organs was higher than unity that suggests that amixin rapidly and reversibly was distributed into these organs from blood. We demonstrate that amixin accumulated in the spleen throughout 24-h period after administration by either oral or intravenous route. This is in agreement with previously reported data on the distribution of tilorone in lymphoid organs [14, 15]. During the first 60 min, the route of administration significantly affected amount of amixin in the spleen that were three- to fivefold higher in the case of intravenous administration.

In the present study, we proposed a variant of the method for determination of K_p described in our previous papers [42, 43]. Derivation of the equilibrium constant of the mass transfer between organs and blood, demonstrated that the use of such integral values as area under the curve of xenobiotic concentration (from 0 to t) gave an unbiased estimation of the mass transfer in contrast to the case when xenobiotic concentration ratios in blood and organs at various time points are used. The suggested integral parameter does not depend on the structure of the kinetic scheme and, most importantly, can be used for analysis of incomplete kinetic curves. Thus, it can be used in the case of the xenobiotic mass transfer in conditions of a poorly defined shape of the kinetic curve, which lacks some phase (absorption, distribution or elimination) during the interval of observation. In our case, such examples were contents of amixin in the brain, spleen and skeletal muscles following oral administration. It should be noted that the suggested analysis of the amixin distribution using total radioactivity is applicable only to studies of drugs with insignificant biotransformation in the body. For substances that undergo intensive metabolism, it would be necessary to study pharmacokinetics of both the original drug and its metabolites with the subsequent use of combined models. The applicability of this formal approach has been practically validated on the example of the distribution of amixin in mice after different ways of its administration. On the basis of this approach, we proposed a combined model that can help to determine parameters of irreversible binding of xenobiotics in mice, the extent of the absorption from

the intestine, relative efficacy of the hepatic excretion, and in particular presystemic elimination of drugs.

References:

1. Algarra I, Perez M, Hoglund P, Gaforio JJ, Ljunggren HG, Garrido F: Generation and control of metastasis in experimental tumor systems; inhibition of experimental metastases by a tilorone analogue. *Int J Cancer*, 1993, 54, 518–523.
2. Algarra I, Gonzalez A, Perez M, Gaforio JJ, Garrido F: Effect of *in vivo* activation of natural killer (NK) cells by a tilorone analogue on the survival of mice injected intravenously with different experimental murine tumours. *Clin Exp Immunol*, 1996, 103, 499–505.
3. Algarra I, Ortega E, Serrano MJ, Alvarez de Cienfuegos G, Gaforio JJ: Suppression of splenic macrophage *Candida albicans* phagocytosis following *in vivo* depletion of natural killer cells in immunocompetent BALB/c mice and T-cell-deficient nude mice. *FEMS Immunol Med Microbiol*, 2002, 33, 159–163.
4. Anderson AL, Banks KE, Pontoglio M, Yaniv M: Alpha/beta interferon differentially modulates the clearance of cytoplasmic encapsidated replication intermediates and nuclear covalently closed circular hepatitis B virus (HBV) DNA from the livers of hepatocyte nuclear factor 1alpha-null HBV transgenic mice. *J Virol*, 2005, 79, 11045–11052.
5. Basley WA, Rees RC, Greager JA, Baldwin RW: Antitumour effects of tilorone hydrochloride on the *in vivo* growth of chemically induced and spontaneously arising rat tumours. *Chemotherapy*, 1981, 27, 44–47.
6. Bazarbachi A, Ghez D, Lepelletier Y, Nasr R, de The H, El-Sabban ME, Hermine O: New therapeutic approaches for adult T-cell leukaemia. *Lancet Oncol*, 2004, 5, 664–672.
7. Bredehorn T, Duncker GI: Tilorone-induced functional changes in the rat retina (German). *Klin Monatsbl Augenheilkd*, 2000, 216, 219–222.
8. Chandra P, Zunino F, Gaur VP: Mode of tilorone hydrochloride interaction to DNA and polydeoxyribonucleotides. *Inst Ther Biochem*, 1972, 28, 5–9.
9. Chandra P, Zunino F, Zaccara A, Wacker A, Goetz A: Influence of tilorone hydrochloride on the secondary structure and template activity of DNA. *Inst Ther Biochem*, 1972, 23, 145–148.
10. Chandra P, Woltersdorf M: Tilorone hydrochloride – a specific probe for A-T regions of duplex deoxyribonucleic acid. *Biochem Pharmacol*, 1976, 25, 877–880.
11. Chen KX: Energetics and stereochemistry of DNA complexation with the antitumor AT specific intercalators tilorone and m-AMSA. *Nucleic Acids Res*, 1988, 16, 3061–3073.
12. Chung JG, Chang HL, Yeh CC, Lu HF, Chang CC, Tsai HD: Effects of the immunomodulator tilorone on the acetylation of 2-aminofluorene and DNA-2-aminofluorene adducts in the rats. *Anticancer Res*, 2000, 20, 467–473.
13. Ershov FI: Amixin application in the therapy of acute and chronic viral infections (Russian). *Medicine*, Moscow, 1998.
14. Fillipova TO, Chudotvorova IG: Peculiarity of accumulation ³H-amixin in lymphoid organs of mice (Ukrainian). *Drug of Ukraine*, 2005, 4, 17–19.
15. Gaur V, Chandra P: Subcellular distribution of ¹⁴C-tilorone hydrochloride in tissues of mice and rats. *Naturwissenschaften*, 1973, 60, 263.
16. Gibaldi M, Perrier D: *Pharmacokinetics*. Ed. Marcel Dekker Inc., New York/Basel, 1982.
17. Grigorian SS, Ivanova AM, Ershov FI: The antiviral activity of amixin and its effect on the interferon status in hepatitis in mice (Russian). *Vopr Virusol*, 1990, 35, 138–140.
18. Grigorian SS, Ivanova AM, Khodzhaev ShKh, Ershov FI: Interferon-inducing activity of amixin and its effect on the interferon status (Russian). *Vopr Virusol*, 1990, 35, 61–64.
19. Golovenko NY, Borisjuk IY: Pharmacokinetics of amixin after repeated peroral administration to mice. *Bull Exp Biol Med*, 2005, 140, 708–710.
20. Hiyama Y, Kuriyama K: Dissociation between anti-inflammatory action of tilorone and its interferon inducing activity. *Agents Actions*, 1991, 33, 229–232.
21. Karpov OV: Thermal denaturation of molecular complexes formed by single stranded RNA with tilorone (Ukrainian). *Ukr Biokhim Zh*, 1997, 69, 49–52.
22. Karpov AV, Zholobak NM, Spivak NY, Rybalko SL, Antonenko SV, Krivokhatskaya LD: Virus-inhibitory effect of a yeast RNA-tilorone molecular complex in cell cultures. *Acta Virol*, 2001, 45, 181–184.
23. Levy L, Aizer F: A dual effect of tilorone on multiplication of *Mycobacterium leprae* in mice. *Agents Actions*, 1984, 15, 398–402.
24. Mezenciwa MV, Narovlyanski AP: Prognoses of efficacy of interferon therapy in different pathology (Russian). *Immunology*, 2001, 4, 41–43.
25. Ortega E, Algarra I, Serrano MJ, de Pablo MA, Alvarez de Cienfuegos G, Gaforio JJ: Enhanced resistance to experimental systemic candidiasis in tilorone-treated mice. *FEMS Immunol Med Microbiol*, 2000, 28, 283–289.
26. Papatheodoridis GV, Hadziyannis SJ: Review article: current management of chronic hepatitis B. *Aliment Pharmacol Ther*, 2004, 19, 25–37.
27. Pisa P, Sitnicka E, Hansson M: Activated natural killer cells suppress myelopoiesis in mice with severe combined immunodeficiency. *Scand J Immunol*, 1993, 37, 529–532.
28. Ruf IK, Lackey KA, Warudkar S, Sample JT: Protection from interferon-induced apoptosis by Epstein-Barr virus small RNAs is not mediated by inhibition of PKR. *J Virol*, 2005, 79, 14562–14569.
29. Salcedo M, Andersson M, Lemieux S, Van Kaer L, Chambers BJ, Ljunggren HG: Fine tuning of natural killer cell specificity and maintenance of self tolerance in MHC class I-deficient mice. *Eur J Immunol*, 1998, 28, 1315–1321.

30. Schultz RM, Howbert JJ, Archer RA: Potent inhibition of interleukin 1 beta-mediated human melanoma (A375.6) lysis by corticosteroids, staurosporine, and tilorone. *Immunopharmacol Immunotoxicol*, 1989, 11, 489–506.
31. Selkova EP, Semenenko TA, Nosik N, Iudina TI, Amarian MP, Lavrukhina LA, Pantiukhova TN, Tarasova Glu: Effect of amixine – a domestic analog of tilorone on characteristics of interferon and immune status of man (Russian). *Zh Mikrobiol Epidemiol Immunobiol*, 2001, 4, 31–35.
32. Selkova EP, Tur'ianov MC, Pantiukhova TN, Nikitina GI, Semenenko TA: Evaluation of amixine reactivity and efficacy for prophylaxis of acute respiratory tract infections (Russian). *Antibiotic Khimioterapiya*, 2001, 46, 4–18.
33. Semenenko TA, Selkova EP, Nikitina GY, Gotvyanskaya TP, Yudina TI, Amaryan MP, Nosik NN, Turyanov MH: Immunomodulators in the prevention of acute respiratory viral infections. *Russ J Immunol*, 2002, 7, 105–114.
34. Smejkal F, Zelena D, Krepelka J, Vancurova I: Derivatives of benzo(c)fluorene. VI. Antiviral and interferon-inducing activities of three benzo(c)fluorenone derivatives in mice. *Acta Virol*, 1985, 29, 11–18.
35. Sokolova TM, Uryvaev LV, Tazulakhova EB, Ershov FI, Malysheva IK, Didkovskii NA: Individual changes of gene expression in the interferon system in human blood cells due to amixin and cycloferon (Russian). *Vopr Virusol*, 2005, 50, 32–36.
36. Soloviev VN, Firsov AA, Filov VA: Pharmacokinetics (Russian). *Medicine*, Moscow, 1980.
37. Sturn J, Srieber L, Daune M: Binding of ligands to a one-dimensional heterogeneous lattice II. Intercalation of tilorone with DNA and polynucleotide. *Biopolymers*, 1981, 20, 765–782.
38. Tazulakhova EB, Parshina OV, Guseva TS, Ershov FI: Russian experience in screening, analysis, and clinical application of novel interferon inducers. *J Interferon Cytokine Res*, 2001, 21, 65–73.
39. Xu D, Erickson S, Szeps M, Gruber A, Sangfelt O, Einhorn S, Pisa P, Grander D: Interferon alpha down-regulates telomerase reverse transcriptase and telomerase activity in human malignant and nonmalignant hematopoietic cells. *Blood*, 2000, 96, 4313–4318.
40. Zakirov IG: Use of amixin in the therapy and prevention of some viral infections (Russian). *Klin Med*, 2002, 80, 54–56.
41. Zhuk OV, Maltsev GV, Sumriy SK: The synthesis and pharmacokinetics of ³H-amixin, a low molecular weight synthetic interferon inductor, in experimental animals. *Drugs Future*, 2002, 27, Suppl 1, 549.
42. Zinkovsky VG, Schukin SI: Approach to model-independent method for analysis of disposition of xenobiotics between the blood and tissue under its administration in a single dose (Ukrainian). *Attainment of the Biology and Medicine*, 2005, 2, 27–32.
43. Zinkovsky VG, Zhuk OV, Golovenko NYa, Schukin SI, Kolesnikov AV: Pharmacokinetics of amixin in organisms. In: *Pharmacological Analysis of the Receptor-Ligand Interactions* (Ukrainian). Akademperiodic, Kiev, 2001, 10–21.
44. Zholobak NM, Mandzhos AP, Verevka SV, Povodzinskii VM, Karpov AV: Interferonogenic activity of immobilized ribopolynucleotides *in vitro* (Ukrainian). *Ukr Biochim Zh*, 2003, 75, 106–110.
45. Wacker A, Lodemann E, Gaur V, Diederich J: Distribution of ¹⁴C-tilorone in mice. *Naturwissenschaften*, 1972, 59, 520.
46. Wang C, Pflugheber J, Sumpter R Jr, Sodora DL, Hui D, Sen GC, Gale MJ: Alpha interferon induces distinct translational control programs to suppress hepatitis C virus RNA replication. *J Virol*, 2003, 77, 3898–3912.
47. Varfalomejev SD, Gurevich KG: *Biokinetics. Practical course* (Russian). Faer-Press, Moscow, 1999.

Received:

February 6, 2007; in revised form: November 12, 2007.